Catalysis Today 155 (2010) 289–295

Contents lists available at ScienceDirect

Catalysis Today

journal homepage: www.elsevier.com/locate/cattod

Combined XRD and XANES studies of a Re-promoted Co/γ-Al_2O_3 catalyst at Fischer–Tropsch synthesis conditions

Magnus Rønning [a,*], Nikolaos E. Tsakoumis [a], Alexey Voronov [a], Rune E. Johnsen [c], Poul Norby [c,d], Wouter van Beek [e,f], Øyvind Borg [b], Erling Rytter [a,b], Anders Holmen [a]

[a] Department of Chemical Engineering, Norwegian University of Science and Technology (NTNU), NO-7491 Trondheim, Norway
[b] Statoil R&D, Research Centre, Postuttak, NO-7005 Trondheim, Norway
[c] Centre for Materials Science and Nanotechnology and Department of Chemistry, University of Oslo, P.O. Box 1033, NO-0315 Oslo, Norway
[d] Present address: Technical University of Denmark, Risø National Laboratory for Sustainable Energy, P.O. Box 49, 4000 Roskilde, Denmark
[e] The Swiss-Norwegian Beam Lines (SNBL) at ESRF, BP 220, F-38043 Grenoble, France
[f] Dipartimento di Scienze e Tecnologie Avanzate, Universita del Piemonte Orientale, A. Avogadro, Viale T. Michel 11, I-15121, Alessandria, Italy

ARTICLE INFO

Article history:
Available online 24 November 2009

Keywords:
Fischer–Tropsch synthesis
Cobalt
In situ
XRD
XANES
XAS
Catalyst deactivation

ABSTRACT

A cobalt based Fischer–Tropsch catalyst was studied during the initial stages of the reaction at industrially relevant conditions. The catalyst consists of 20 wt% cobalt supported on γ-Al_2O_3 and promoted by 1 wt% of rhenium. X-ray diffraction (XRD) in combination with X-ray absorption near edge structure (XANES) were used to reveal information on the particle and crystallite size and the oxidation states of the active component. Conditions giving high selectivity towards light hydrocarbons (methanation, 673 K, 10 bar and high GHSV) were compared to conditions were higher hydrocarbons are the main products (FT synthesis at 483 K, 18 bar and low GHSV). The data analysis shows no significant changes in the cobalt crystallites during the first hours of Fischer–Tropsch synthesis. Running the reaction at higher temperatures and predominantly methanation conditions led to significant sintering of the cobalt particles and a further reduction of a partially reduced catalyst could be observed.

1. Introduction

The Fischer–Tropsch synthesis (FTS) is an important part of recent natural gas conversion process developments. Modern Fischer–Tropsch synthesis aims at converting synthesis gas into high quality diesel. A key element in improved Fischer–Tropsch technology is the development of active and stable catalysts with high selectivity towards wax. Cobalt is considered as the most favourable metal for the synthesis of long-chain hydrocarbons from natural gas [1]. Cobalt demonstrates good characteristics in terms of conversion per pass and selectivity. Addition of small amounts of a noble metal is beneficial for the synthesis. It is known that rhenium addition mainly enhances catalysts reducibility and increases dispersion [2]. However, catalyst deactivation is an inevitable challenge in most catalytic reactions including Fischer–Tropsch synthesis. Thus, catalyst stability is an important factor for the industrial exploitation of the process.

Various mechanisms for catalyst deactivation have been proposed including reoxidation of active sites [3–5], polymeric surface carbon formation [6], sintering [7–10] and surface metal-support compound formation [11]. Catalyst poisoning from impurities in the catalyst as well as from the feed may also result in catalyst deactivation [12]. Mechanical degradation of the catalyst through attrition is also a topic of scientific interest [13]. Poisoning and attrition may be partially controlled by feed purification and reactor design. The other possible deactivation mechanisms are directly related to the chemical environment surrounding the catalyst. The activity loss is strongly interrelated with the product selectivity and the conversion level. Different deactivation mechanisms may dominate depending on the selected conditions, and the cause of deactivation should be examined in connection with the abundance (partial pressures) of products and intermediates. A large number of studies on the effect of water, which is the most abundant by-product, have been published and reviewed [14,15]. However, the majority of the studies are performed by co-feeding water to mimic high conversion instead of using true FTS conditions.

In practice, studies of FT catalyst deactivation are performed on spent catalysts removed from the reactor after a certain time on stream (TOS). This procedure involves several steps including sampling, dewaxing and characterisation. All steps need to be performed at inert conditions in order to avoid exposure of the active Co phase to air. Furthermore, the large amount of hydrocarbon waxes covering the surface is also limiting the

* Corresponding author.
E-mail address: ronning@chemeng.ntnu.no (M. Rønning).

0920-5861/$ – see front matter © 2009 Elsevier B.V. All rights reserved.
doi:10.1016/j.cattod.2009.10.010

number of useful characterisation techniques. Hence, *in situ* characterisation techniques that are capable of providing information about the catalyst under realistic working conditions are necessary and essentially the only way to obtain accurate information about the active phase of the catalyst at industrially relevant conditions.

Realistic FT conditions imply temperatures in the range of 473–523 K and a pressure well above ambient [16]. Furthermore, the feed conveniently can be concentrated syngas with H_2/CO at the usage ratio of 2.1. The conversion level should be high (~50%) with a corresponding high selectivity towards C_{5+} hydrocarbons. The characterisation techniques need to be able to operate at these conditions. In addition, they should be able to distinguish the active phase from the support and from the produced wax. Since catalyst activation (reduction) and deactivation may involve transient phenomena, there is also a persistent trade-off between time resolution and data quality.

From these constrains, two techniques were selected for the detection of potential sintering and reoxidation of the catalyst during the initial stages of the reaction [17,18]. The techniques are X-ray diffraction (XRD) and X-ray absorption spectroscopy (XAS) using synchrotron radiation. de Smit et al. recently combined XAS and wide angle X-ray scattering (WAXS) on iron based FT catalysts [19] at 1 bar and up to 723 K. In the present work, the data acquisition has been performed *in situ* at industrially relevant conditions (18–20 bar, 483 K) with simultaneous product analysis using an on-line mass spectrometer (MS). The changes in the catalyst crystallites were investigated during the initial stages of the FT reaction until steady state conditions were established.

A rhenium promoted cobalt catalyst, supported on γ-Al_2O_3 has been characterised by XRD and XAS in an *in situ* cell similar to that described by Clausen et al. [20]. The cell resembles a laboratory plug flow reactor (PFR) since the catalyst is packed in a 1 mm diameter quartz capillary tube. A gas feeding system dedicated for *in situ* studies in a controlled environment has been installed at the Swiss-Norwegian Beamlines (SNBL) at the ESRF. The system is especially designed for *in situ* XAS and XRD studies of catalysts and consists of a delivery system (valves and mass flow controllers) and a portable switching system which can be connected to the experimental cells for either XRD or XAS measurements. The system is designed to be able to operate at pressures up to 20 bar using a wide range of reaction gases. During the initial stages of the reaction, no reoxidation or sintering of the Co catalysts are detected.

2. Experimental

The *in situ* experiments were performed at the Swiss-Norwegian Beamlines (SNBL) at the European Synchrotron Radiation Facility (ESRF) in France. Both beamline stations BM01A (multipurpose image plate detector) and BM01B (combined high-resolution powder XRD and XAS) were used.

2.1. Catalyst preparation

The catalyst used in this study consists of 20 wt% Co and 1 wt% Re supported on γ-Al_2O_3. The catalyst was prepared by co-impregnation of $Co(NO_3)_2{\cdot}6H_2O$ and $HReO_4$ to give 20% Co and 1% Re. The catalyst was dried in air at 393 K for 3 h and calcined in air at 573 K for 16 h. The catalyst was sieved to particle sizes of 53–90 μm [2,18].

2.2. Hydrogen chemisorption

Hydrogen adsorption isotherms were recorded on a Micromeritics ASAP 2010 unit at 313 K [2]. The sample (0.3–0.5 g) was evacuated at 313 K for 1 h, and then reduced in flowing hydrogen at 623 K for 16 h. The temperature was increased at 1 K/min from 313 to 623 K. After reduction, the sample was evacuated for 1 h at 603 K and for 30 min at 373 K before subsequent cooling to 313 K. Adsorption isotherms were recorded at this temperature in the pressure interval 20–510 mmHg. Chemisorption isotherms were extrapolated to zero pressure and the amount of chemisorbed hydrogen was determined by the straight-line portion of the isotherm difference. Furthermore, in order to calculate the dispersion, it was assumed that two cobalt sites are covered by one hydrogen molecule [21], and that rhenium does not contribute to the amount of hydrogen adsorbed [22]. The cobalt metal particle size ($d(Co^0)$ nm) was calculated from the cobalt metal dispersion (D, %) by assuming spherical, uniform cobalt metal particles with site density of 14.6 atoms/nm^2. These assumptions give the following formula:

$$d(Co^0)\ (\text{nm}) = 96/D\ (\%) \quad (1)$$

2.3. Combined XAS and high-resolution powder XRD experiments

High-resolution X-ray powder diffraction (XRD) measurements were performed simultaneously with XAS measurements at the BM01B station of the Swiss-Norwegian Beamlines (SNBL) using two independent Si(1 1 1) monochromators. The beam current varied in a range of 100–200 mA at 6.0 GeV.

The high-resolution XRD data were collected with the standard BM01B setup, using a wavelength of 0.8007 Å [23]. The applied slits provided an X-ray beam spot of 4 mm horizontal size and 0.6 mm vertical size at the sample position. The high-resolution diffractometer is equipped with an X-ray detector consisting of six independent counting chains, each made of a Si(1 1 1) analyser crystal and a NaI scintillation counter. Data were collected for angles in the range from 9° to 30° throughout catalyst treatment and testing. Acquisition time for each diffractogram was 19.1 min.

XAS spectra were recorded at the cobalt K edge (E = 7709 eV, λ = 1.6086 Å) using a double crystal Si(1 1 1) monochromator. The data collection was carried out in transmission mode. Ion chamber detectors with their gases at ambient temperature and pressure were used for measuring the intensities of the incident (I_0) and transmitted (I_t) X-rays. The samples were mixed with the required amount of boron nitride (Alfa Aesar 99.5% CAS: 10043-11-5) to achieve the desired absorber thickness. The optimal ratio between catalyst and diluent (BN) in the combined experiments was chosen by a series of test measurements. Capillaries with different catalyst dilution were checked in order to obtain samples of good absorber thickness (2–3 absorption lengths) that simultaneously displayed acceptable XRD patterns. A cobalt metal foil, CoO and Co_3O_4 powders were used as XAS references. The energy calibration was checked by measuring the spectrum of the cobalt foil with the energy of the first inflection point being defined as the edge energy (7709 eV).

2.4. Image plate (MAR345) XRD experiments

In order to increase the signal to noise and hence the time resolution of the data collection, XRD measurements were performed at beamline station BM01A. Powder diffraction data were collected using a MAR345 area detector of 345 mm diameter and focusing optics. A wavelength of 0.70417 Å, a sample-to-detector distance of 229.03 mm and an exposure time of 30 s was used. This resulted in a time resolution of 101.46 s per scan (exposure time + data readout time). The data were converted to normal one-dimensional powder patterns using the program FIT2D [24].

2.5. XRD data analysis

The WinPLOTR software (April 2008) of the FullProf suite was used for profile fitting and acquisition of the FWHM. The cobalt crystallite sizes have been estimated using the Scherrer formula. Assuming uniform and spherical crystallites a geometrical factor of 4/3 was applied to the crystallite size [25]. A K factor of 0.89 was used and instrumental line broadening was assumed to be insignificant for the high-resolution XRD from BM01B, and estimated to be 0.12° for BM01A using a LaB_6 standard.

2.6. XAS data analysis

The Athena software from the Ifeffit software package (Version 1.2.9) [26] was used for the XAS data analysis. The identification of the Co phases present during *in situ* reduction was done by a linear combination (LC) of the XANES spectra. Reference spectra were used in a fitting procedure to determine the quantity of each phase present. Spectra from the freshly calcined sample were used as a reference for the Co_3O_4 whereas cobalt foil was used as Co(0) reference and a powder sample of pure CoO as the Co^{2+} reference. The algorithm uses a least squares procedure to refine the sum of a given number of reference spectra to the experimental spectrum.

2.7. The in situ cell

An *in situ* cell [20] was used in order to combine the X-ray techniques and FT reaction at realistic reaction conditions. The cell consists of a stainless steel base and two linear motion guides. The standard Swagelok 1/8 in. unions are fixed at a 45° angle in order to prevent liquid products accumulation inside the cell. A condenser tank was installed to collect the liquid products. All the cell parts were made from stainless steel. A quartz capillary tube was used as a microscale reactor for the *in situ* studies of the FTS. The capillary dimensions are the following: length = 60 mm, outer diameter = 1 mm, wall thickness = 0.02 mm. The catalyst bed length was limited to 10 mm and kept in place inside the quartz tube by quartz wool plugs. The sample was heated by a vertical hot air blower. The heat blower nozzle diameter was 12 mm. Blower calibration has been done with the use of thermal expansion of silver in a Ag-Si reference sample.

Gas flows were supplied by the gas distribution system at SNBL. Gas flows were controlled by Bronkhorst mass flow controllers and the pressure was maintained by a Bronkhorst pressure controller (range 1–20 bar). A carbonyl trap was installed directly after the CO bottle and before the mass flow controller to prevent contaminations from metal carbonyls.

2.8. Catalyst reduction

The pretreatment of the catalyst was done *in situ*. Two reduction profiles were used as described in Table 1. One reduction took place at 673 K and the other at 723 K. In both cases the sample was exposed to a pure hydrogen flow of 2.5 ml/min at ambient pressure, while the temperature was increased from 298 K to the desired set-point at a heating rate of 3 K/min. The temperature was held at the set-point for 4 h before returning to 443 K under flowing He (5 ml/min).

Table 1
Catalyst pretreatment (reduction).

Experiment	Ramp rate [K/min]	Temperature set-point [K]	H_2 flow [ml/min]	wt% of BN	GHSV [Nl/catg h]
FT0	3	723	2.5	50%	53
FT1	3	673	2.5	–	26
FT2	3	673	2.5	–	26
FT3	3	673	5	25%	65

Boron nitride (BN) is used as a dilutor for optimising the absorber thickness (see Section 2). The temperature was kept at the set-point for 4 h for all experiments.

Table 2
Summary of the reaction conditions during the experiments.

Experiment	Conditions			
	Pressure [bar]	Temperature [K]	GHSV [Nl/catg h]	Duration [h]
FT1	10	483–673	131	2 + 1.5[a]
FT2	10	483–673	97	2 + 1.5[a]
FT3	18	483	8	6

[a] 2 h at 483 K and 1.5 h elevating and staying at 673 K. H_2/CO ratio kept constant at 2.1 for all experiments.

2.9. Fischer–Tropsch synthesis

After reduction the temperature was lowered to 443 K before pressurising the reactor in synthesis gas (H_2:CO = 2.1). When the desired reaction pressure was reached, the temperature was slowly increased to 483 K. The reaction was allowed to run for several hours until stable conversion. After some hours of reaction the temperature was increased and kept at 673 K for 1 h. The experimental conditions are summarised in Table 2.

3. Results and discussion

This study focuses on detecting changes in Co oxidation state and crystallite size that may occur during the initial stages of the Fischer–Tropsch reactions at industrially relevant conditions. The catalyst had a Co dispersion of 6–9% depending on which technique the number was determined from (chemisorption and XRD). This corresponds to a Co particle size of 11–16 nm (see Table 3).

Fig. 1 shows the diffractograms of the relevant cobalt phases. During reduction the cobalt is transformed from the Co_3O_4 spinel structure of the freshly calcined catalyst, via the metastable CoO before the final formation of Co^0 (fcc and hcp). This evolution has an influence on the size of the Co crystallites. It has been reported [27] that heating rate and composition of the reducing gas mixture

Table 3
Dispersion, particle size and extent of reduction for the catalyst.

Catalyst	H_2 chemisorption		XRD		XANES
	Dispersion[a] [%]	Crystallite size[b] [nm]	Crystallite size[c] [nm]	Dispersion[d] [%]	DOR[e] [%]
20%Co1%Re/γ-Al_2O_3	5.9	16.4	10.7	8.9	90

[a] Cobalt metal dispersion from H_2 chemisorption at 313 K, assuming adsorption on Co atoms only.
[b] Cobalt metal crystallite size calculated from H_2 chemisorption using $d(\mathrm{Co}) = 96/D$.
[c] Cobalt metal crystallite size calculated from XRD of reduced catalyst.
[d] Cobalt metal dispersion calculated from XRD data, using the relation $D = 96/d(\mathrm{Co})$.
[e] Degree of reduction calculated from linear combination of XANES spectra.

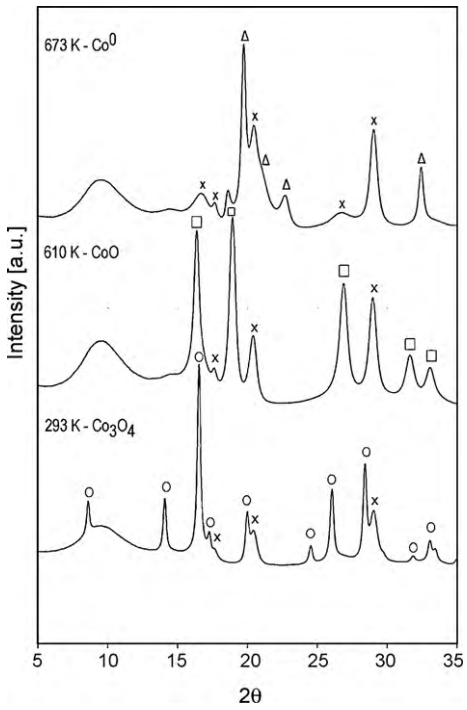

Fig. 1. Selected diffractograms from the start of the reduction (293 K) experiment FT1. The transition phase (610 K) and at the end of the reduction (673 K) ((○) Co_3O_4, (□) CoO, (×) support and (△) fcc and hcp metallic cobalt). λ = 0.70417 Å.

may influence the final particle size distribution. During reduction these phase transitions can be monitored with the use of XRD with sufficient time resolution. The transitions are presented in a 3D plot in Fig. 2 showing the changes in intensity of the most intense peaks at ~16.54° 2θ for Co_3O_4, ~18.93° 2θ for CoO and ~20.44° 2θ for the metallic cobalt. Rhenium is highly dispersed in the catalysts and the relatively low loading is not sufficient for rhenium phases to be detected in XRD.

X-ray line broadening analysis (LBA) using the Scherrer equation was applied to selected diffractograms during reduction. The selection of the diffractograms was done with respect to maximum intensity of each phase to minimize interference from overlapping peaks. The crystallite sizes obtained from the LBA are presented in Table 4.

From the Scherrer sizes, it appears that the metallic cobalt crystallites after reduction are reduced in size by approximately 40% compared to the initial phase. The crystallite size is expected

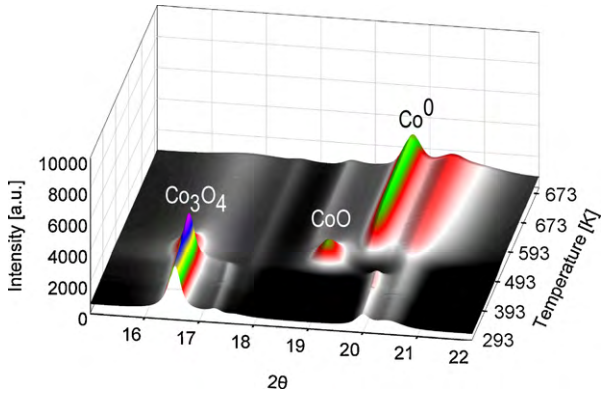

Fig. 2. The phase transition from Co_3O_4 via CoO to obtain the metallic cobalt monitored by XRD during reduction of the FT catalyst (experiment FT1, 250 scans). λ = 0.70417 Å.

Table 4
Cobalt crystallite sizes during reduction (exp. FT1).

Cobalt phase	Crystallite size[a] [nm]	Temperature [K]
Co_3O_4	17.8	293
CoO	9.9	610
Co^0	10.7	673

[a] Crystallite size calculated from XRD using the Scherrer equation assuming spherical shape.

to decrease due to loss of oxygen. Cobalt (ccp) has a unit cell with edge length a = 3.544 Å and number of formula units Z = 4 [28]. Thus the volume of this cubic cell will be $V_{\text{unitcell}} = abc(1 - \cos^2\alpha - \cos^2\beta - \cos^2\gamma + 2\cos\alpha\cos\alpha\cos\gamma)^{1/2}$ = 44.51 Å^3 and the volume per cobalt atom is V/(number of Co atoms in the unit cell) = 11.12 Å^3/Co atom. Equally the Co_3O_4 spinel structure has edge length of a = 8.065 Å and number of formula units Z = 8, while it contains three atoms of cobalt in the formula [29]. The volume of the cubic cell will thus be V = 524.58 Å^3 and the volume normalised per cobalt atom gives 21.858 Å^3/Co atom. By introducing the assumption of spherical cobalt crystallites, the equation $V_{\text{sphere}} = \pi d^3/6$ which corresponds to the volume of a sphere can be applied for both crystals. Solving the equation with respect to crystallite diameters gives $d(Co_{ccp}) = 0.80\, d(Co_3O_4)$. The value will not change significantly for the various close packing configurations of the metallic state (fcc, hcp or hcp–fcc intergrown phases). The XANES data of the same sample after reduction show a degree of reduction (DOR) in the range of 90% (Table 2). The DOR (i.e. the fraction of Co in the metallic state) was determined by linear combination of XANES. Thus, domains of CoO in the metallic cobalt particles may reduce the calculated Scherrer size of the cobalt crystallites. Redispersion of cobalt crystallites during reduction can not be excluded. In contrast, all the Co_3O_4 is transformed. Thus, the relatively small size of the CoO crystallites cannot be explained solely by the existence of larger domains of Co^{3+}-containing oxide inside the CoO particles. Williamson–Hall plots [30] indicate that the Co_3O_4 and CoO phases contain a significant amount of strain. Hence, the sample-dependent broadening of the diffraction peaks is most likely not purely due to finite crystallites. Stacking faults in the metallic cobalt phases, as suggested by Ducreux et al. [31] may also have contributed to the broadening of the diffraction peaks. The existence of other sample-dependent broadening effects implies that the crystallite sizes calculated from the Scherrer equation will be underestimated.

3.1. In situ XRD during FT synthesis

Sintering of cobalt crystallites during FTS has been proposed as a possible explanation for the activity loss experienced by FT catalysts in the early stages of the reaction [7–9]. This early stage ranges from a few hours up to several months on stream. The reported studies include information from XRD, EXAFS and TEM techniques obtained from used samples that have been preserved in the active state. This procedure involves catalyst sampling from the reactor either in a sequential way or by shutting down the process at various stages. In addition it is assumed that wax covering the catalyst surface protects the catalyst from being exposed to air. In most cases an inert protection is applied during unloading. However, this is a critical step due to the pyrophoric properties of metallic cobalt. A fraction may be immediately oxidised leading to unreliable determination of particle size and degree of oxidation.

FTS has been studied *in situ* by XRD at a pressure of 10 bar. The experiments were performed with two temperature set-points. Initially the reaction was carried out at 463 K before being raised to 673 K. The reaction was run for 4 h at 10 bar and relatively high space velocity (>90 Nl/gcat h). The methane formation was

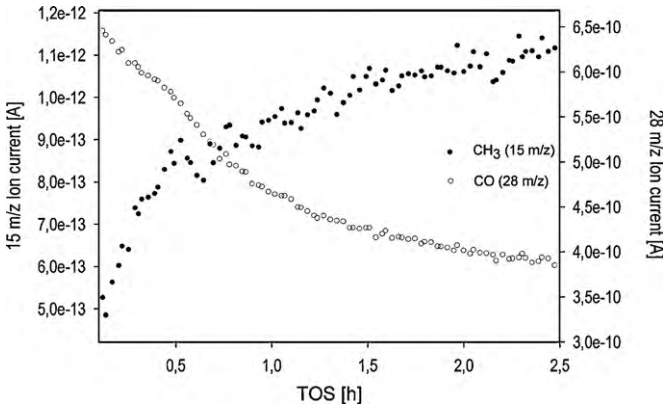

Fig. 3. MS signal during the first hours of experiment FT2 at 483 K. ((●) 15 *m*/*z* and (○) 28 *m*/*z*).

(qualitatively) monitored by an on-line quadrupole mass spectrometer (MS). The evolution of the 15 *m*/*z* (CH_3) fraction together with the 28 *m*/*z* (CO) was observed. The ion currents during time on stream (TOS) are presented in Fig. 3.

A decrease in CO concentration is observed with a simultaneous increment of the CH_3^+ fragment which confirms hydrocarbon formation. The reaction was followed by time resolved XRD and a 3D plot of the reaction progress is presented in Fig. 4.

No visible changes in the diffraction peaks are detected in the plot in Fig. 4. A closer examination of the diffractograms before reaction and after 2 h reaction is presented in Fig. 5. It shows that the only difference is in the intensity around the broad scattering bump from the capillary at ~9.35° 2θ. This additional scattering intensity is attributed to scattering from the liquid hydrocarbons (wax) accumulating in the reactor at the present conditions.

It appears that the metallic cobalt peaks remain unchanged during this initial stage of the reaction. The calculated crystallite sizes before and at the end of the reaction were both 10.7 nm. A diffractogram of a sample consisting of FT waxes (C_{30+}) taken from a laboratory plug flow reactor was collected using a sealed capillary at the same temperature as for the catalyst. The XRD pattern of the wax displays a similar peak as the XRD pattern of the catalyst during FT reaction (Fig. 5). However the peak in the wax sample is slightly shifted. This may be due to the variation in product distribution and steam partial pressure from the present reaction conditions (not entirely C_{30+}).

FTS was subsequently carried out at 673 K in order to promote methane formation and provoke sintering by increasing the

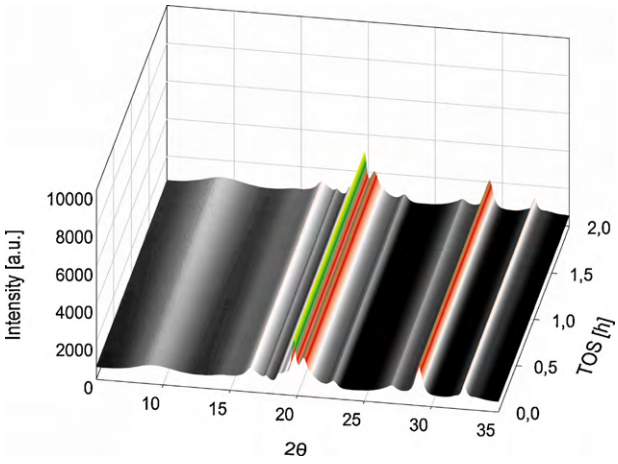

Fig. 4. XRD profiles, during the first 2 h on stream at 493 K, of experiment FT1 consisting 140 scans. λ = 0.70417 Å.

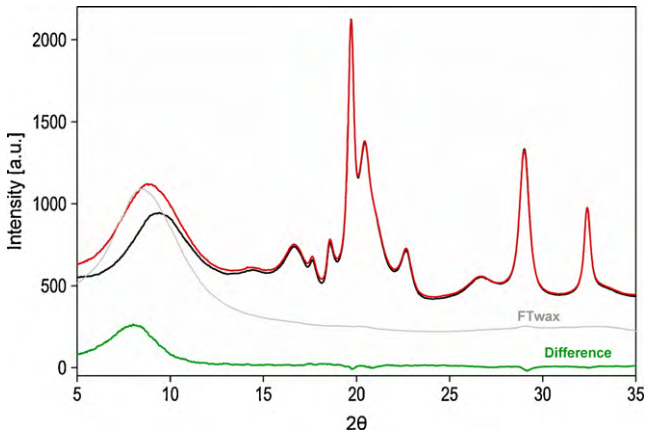

Fig. 5. Diffractograms from the start (black) and after 2 h of FT1 reaction at 483 K (red). The difference curve (green) indicates no significant changes in the Co peaks during reaction compared to scattering from FT wax only (grey) and from the catalyst at the end of the reaction at 483 K (red), λ = 0.70417 Å. (For interpretation of the references to color in this figure legend, the reader is referred to the web version of the article.)

thermal load in the catalyst. After 2 h on stream the temperature was raised to 673 K at a rate of 10 K/min. Data analysis indicates an increase in the Scherrer size of the cobalt crystallites. The size of the cobalt crystallites increased approximately 20% after 1 h of reaction. Particle growth seems to start immediately after the applied conditions are reached.

3.2. FT synthesis at industrially relevant conditions (FT3)

The *in situ* cell was operated at industrially relevant conditions (483 K and 18 bar) for 6 h. The space velocity (GHSV = 7.8 Nl/(gcat h)) was adjusted to give 30–50% CO conversion as previously demonstrated in a laboratory fixed bed reactor [2]. Methane formation was detected qualitatively by means of MS by monitoring the 15 *m*/*z* fragmentation, selected in order to avoid interference with oxygen. In addition, liquid products were detected as an increase in the scattering intensity at lower XRD angles. This is because the liquid products gradually fill the catalyst pores and the reactor during the initial stages of the reaction. Visual inspection of the quartz reactor confirmed liquid products appearing at the outlet of the reactor after a few minutes of reaction. XRD line broadening analysis showed no detectable changes in the cobalt crystallite size during the reaction. This is demonstrated in Fig. 6b. Both the difference curve and the average crystal size show no significant changes in the XRD patterns of the cobalt catalysts. This is in agreement with the results from FT1 that was run at 10 bar for 2 h.

3.3. Oxidation state of cobalt

XANES is a valuable tool for monitoring changes in oxidation states [18]. XANES spectra were recorded during reduction and reaction using the same setup and conditions as for the high-resolution XRD experiments. A comparison of the spectra with the reference compounds shows that cobalt in the catalyst sample before reduction is present as Co_3O_4. During reduction Co_3O_4 is first transformed to CoO and further to metallic cobalt. This is confirmed both by XRD and XANES.

It is evident from the XANES that cobalt oxide is not completely reduced to cobalt metal. According to a linear combination fitting, about 10% of the cobalt remains in the non-metallic phase after reduction for 4 h at 673 K in H_2. The non-metallic residue closely resembles the XANES profile of CoO (Figs. 7 and 8).

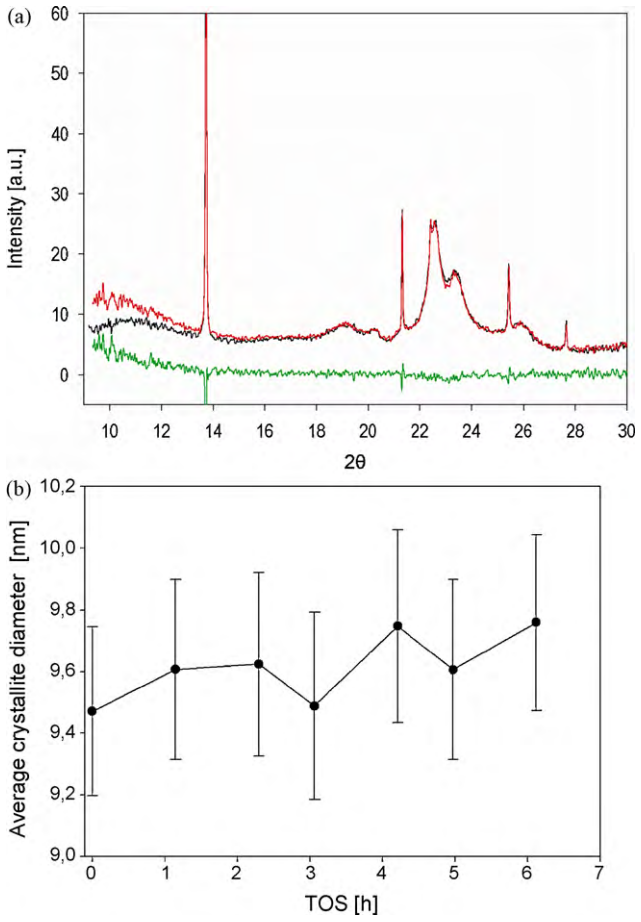

Fig. 6. (a) The difference curve (green) of the two diffractograms collected at the start (black) and at the end of the experiment FT3 (red). The sharp narrow peaks correspond to BN. (b) LBA at different stages of the reaction using the Scherrer equation, λ = 0.8007 Å. (For interpretation of the references to colour in this figure legend, the reader is referred to the web version of the article.)

XANES spectra were also recorded during FT synthesis. No significant changes in the oxidation state of cobalt were detected during 6 h of reaction at 483 K and 18 bar. The catalyst maintained a degree of reduction close to 90%. The XANES profiles during reduction and reaction are presented in Fig. 8.

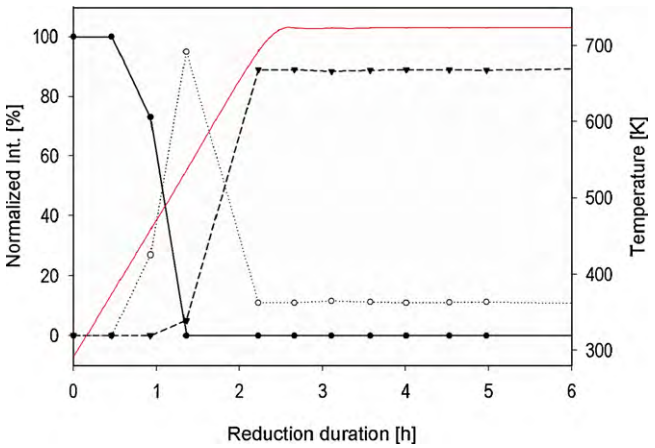

Fig. 7. Cobalt phase composition during reduction (FT0) from the linear combination of XANES ((●) Co_3O_4, (○) CoO, (▼) Co; the red line shows the temperature profile). (For interpretation of the references to colour in this figure legend, the reader is referred to the web version of the article.)

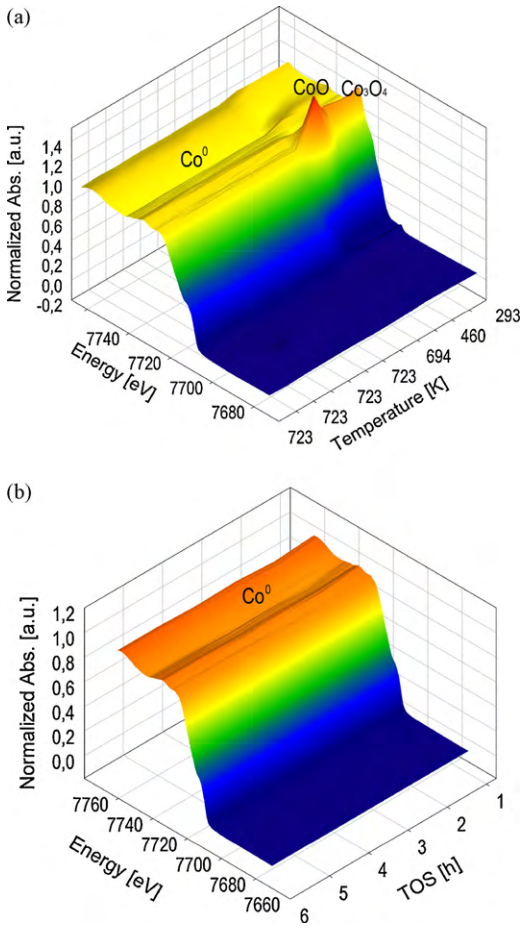

Fig. 8. XANES profiles during reduction (a) and reaction (b) at 18 bar and 483 K. Scans are collected in intervals of approximately 30 min.

The XANES spectra in Fig. 8 show no sign of reoxidation of Co at the applied FT conditions. However, spectra were recorded only in the initial period of the reaction. Results from our fixed bed laboratory reactor suggest that an induction period of approximately 5–6 h is needed in order to obtain steady state conditions in the reactor. Thus, the reaction should be run for an extended period of time in order to detect initial FT deactivation mechanisms.

Since reoxidation is one of several proposed deactivation mechanisms it is of interest to determine if the conditions in the FT reactor is predominantly reducing or oxidising. Hence, a partially reduced catalyst, were the CoO diffraction peaks were clearly visible, was exposed to FT conditions (exp. FT2). A slight decrease

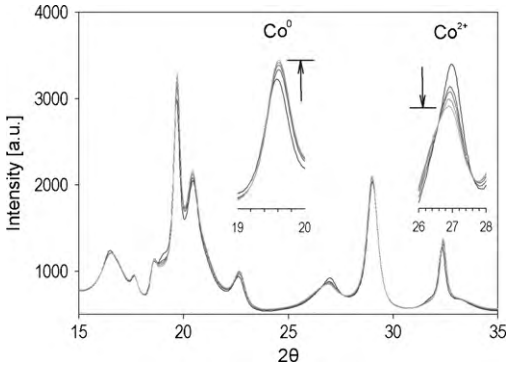

Fig. 9. XRD patterns of a partially reduced catalyst showing a decrease in CoO peak intensity during FT synthesis (FT2) at 673 K.

could be observed in the intensity of the CoO peaks at 673 K in Fig. 9 for the partially reduced catalyst during FT reaction indicating a further reduction of the cobalt catalyst. A significant loss of intensity in the CoO peaks can be seen at 673 K and a corresponding increase in the intensity of the peak assigned to metallic cobalt. A minor increase in the Co crystallite size is also detected. This shows that the reaction takes place in reducing environment when methane is the main product. The effect of the products and conversion level on the possible reoxidation of cobalt will be further examined in a proceeding study.

4. Conclusions

A 20%Co-1%Re/γ-Al_2O_3 catalyst has been characterised in a combined *in situ* XRD-XAS study at realistic Fischer–Tropsch conditions (483 K, 10 and 18 bar). The behaviour of a laboratory plug flow reactor can be simulated in the cell and the conversion level can be monitored using an on-line MS. X-ray techniques were applied in order to detect structural changes in the catalyst during initial stages of the FT synthesis. XRD and XANES are sensitive to structural changes such as crystallite size and oxidation state, respectively. Line broadening analysis of the XRD profiles revealed that at 483 K no significant sintering occurs during the first hours of reaction. At 673 K and under methanation conditions (high temperatures, low pressures and high space velocity) cobalt crystallite particle growth and further reduction of cobalt were observed. A study of the FTS reaction at relevant conditions extending beyond the first 5–6 h is necessary to give further information about the causes of initial deactivation in the FTS.

Acknowledgements

The authors would like to thank the Norwegian Research Council and Statoil for financial support through the inGAP project (Innovative Natural Gas Processes and Products) and acknowledge the personnel of Swiss-Norwegian Beamlines at ESRF for experimental assistance (experiments 01-02-785 and 01-01-759). In particular Olga Safonova is acknowledged for her work on the *in situ* capabilities of the beamline and Geir Wiker at the NTNU mechanical workshop (presently at SNBL) for technical assistance with the *in situ* cell. David S. Wragg is acknowledged for the assistance in the XRD data collection.

References

[1] M.E. Dry, Catal. Today 71 (2002) 227.
[2] Ø. Borg, N. Hammer, S. Eri, O.A. Lindvåg, R. Myrstad, E.A. Blekkan, M. Rønning, E. Rytter, A. Holmen, Catal. Today 142 (2009) 70.
[3] D. Schanke, A.M. Hilmen, E. Bergene, K. Kinnari, E. Rytter, E. Adnanes, A. Holmen, Energy Fuels 10 (1996) 867.
[4] P.J. van Berge, J. van de Loosdrecht, S. Barradas, A.M. van der Kraan, Catal. Today 58 (2000) 321.
[5] G. Jacobs, T.K. Das, Y. Zhang, J. Li, G. Racoillet, B.H. Davis, Appl. Catal. A: Gen. 233 (2002) 263.
[6] D.J. Moodley, J. van de Loosdrecht, A.M. Saib, M.J. Overett, A.K. Datye, J.W. Niemantsverdriet, Appl. Catal. A: Gen. 354 (2009) 102.
[7] C.J. Bertole, C.A. Mims, G. Kiss, J. Catal. 210 (2002) 84.
[8] G. Jacobs, A. Sarkar, Y. Ji, M. Luo, A. Dozier, B.H. Davis, Ind. Eng. Chem. Res. 47 (2008) 672.
[9] M.J. Overett, B. Breedt, E. du Plessis, W. Erasmus, J. van de Loosdrecht, Prepr. Pap. Am. Chem. Soc., Div. Petr. Chem. 53 (2008) 126.
[10] A. Tavasoli, R.M. Malek Abbaslou, A.K. Dalai, Appl. Catal. A: Gen. 346 (2008) 58.
[11] A. Sirijaruphan, A. Horváth, J.G. Goodwin, R. Oukaci, Catal. Lett. 91 (2003) 89.
[12] C.G. Visconti, L. Lietti, P. Forzatti, R. Zennaro, Appl. Catal. A: Gen. 330 (2007) 49.
[13] D. Wei, J.G. Goodwin, R. Oukaci, A.H. Singleton, Appl. Catal. A: Gen. 210 (2001) 137–150.
[14] E.A. Blekkan, Ø. Borg, V. Frøseth, A. Holmen, Catalysis 20 (2007) 13.
[15] A.K. Dalai, B.H. Davis, Appl. Catal. A: Gen. 348 (2008) 1.
[16] A. Steynberg, M. Dry, in: A. Steynberg, M. Dry (Eds.), Studies in Surface Science and Catalysis, vol. 152, Elsevier, 2004, p. 3.
[17] T.K. Das, G. Jacobs, P.M. Patterson, W.A. Conner, J. Li, B.H. Davis, Fuel 82 (2003) 805.
[18] Ø. Borg, M. Rønning, S. Storsæter, W. van Beek, A. Holmen, in: B.H. Davis, M.L. Occelli (Eds.), Studies in Surface Science and Catalysis, vol. 163, Elsevier, 2007, p. 255.
[19] E. de Smit, A.M. Beale, S. Nikitenko, B.M. Weckhuysen, J. Catal. 262 (2009) 244.
[20] J.D. Grunwaldt, B.S. Clausen, Top. Catal. 18 (2002) 37.
[21] R.C. Reuel, C.H. Bartholomew, J. Catal. 85 (1984) 63.
[22] D. Schanke, S. Vada, E.A. Blekkan, A.M. Hilmen, A. Hoff, A. Holmen, J. Catal. 156 (1995) 85.
[23] E. Boccaleri, F. Carniato, G. Croce, D. Viterbo, W. van Beek, H. Emerich, M. Milanesio, J. Appl. Crystallogr. 40 (2007) 684.
[24] A.P. Hammersley, S.O. Svensson, M. Hanfland, A.N. Fitch, D. Hausermann, High Pressure Res. 14 (1996) 235.
[25] J.L. Lemaitre, P. Govind Menon, in: F. Delannay (Ed.), Characterization of Heterogeneous Catalysts, Marcel Drekker Inc., New York, 1984, p. 299.
[26] B. Ravel, M. Newville, Phys. Scripta T115 (2005) 1007.
[27] P.A. Chernavskii, Kinet. Catal. 46 (2005) 634.
[28] W.L. Roth, J. Phys. Chem. Solids 25 (1964) 1.
[29] S. Mueller, P. Scholten, Z. Angew. Phys. 20 (1966) 498.
[30] G.K. Williamson, W.H. Hall, Acta Metall. 1 (1953) 22.
[31] O. Ducreux, B. Rebours, J. Lynch, M. Roy-Auberger, D. Bazin, Oil Gas Sci. Technol. Rev. IFP 64 (2009) 49.